# Si-Shift

High-performant non-oriented electrical steels with a silicon content beyond today's limits: new materials for an electrified future.


## Deliverable D3.1 – Fe-Si phase diagram

Author: Nikitha Srinivasan and Stefaan Cottenier, Ghent University, Belgium

Si-Shift - Project: 101112518 —RFCS-02-2022-RPJ
Start date: 2023-09-01
Duration: 42 months
Project coordinator: Ghent University
Coordinator contact: Stefaan Cottenier, Stefaan.cottenier@ugent.be

**Document information**

| | |
|---|---|
| Project Acronym | Si-Shift |
| Project No. | 101112518 |
| Project Call | RFCS-02-2022-RPJ - Steel Research Projects |
| Title | Fe-Si phase diagram |
| Deliverable no. | 3.1 |
| Draft delivery date | August 31, 2024 |
| Dissemination level | PU |
| Deliverable type | digital report |
| Authors | Nikitha Srinivasan and Stefaan Cottenier |

Document history:

| Version | Date of issue | Content and changes | Edited by |
|---|---|---|---|
| 1.0 | August 29, 2024 | First version | Nikitha Srinivasan<br>Stefaan Cottenier |
| | | | |
| | | | |

Research Fund for Coal & Steel
Funded by the European Union

## Abstract


| Deliverable abstract |
| --- |
| This document reports on a computational assessment of the Fe-rich part of the Fe-Si phase diagram. The computational procedure is presented, as well as the procedure to predict the phase diagram. Three stable phases are found, one of them having not been experimentally recognized before. |

# Contents

## 1 Context and goal

The Fe-Si temperature/composition phase diagram has been studied intensively over the past decades, and has been recently summarized by Han et al. (Journal of Alloys and Compounds 919 (2022) 165810):

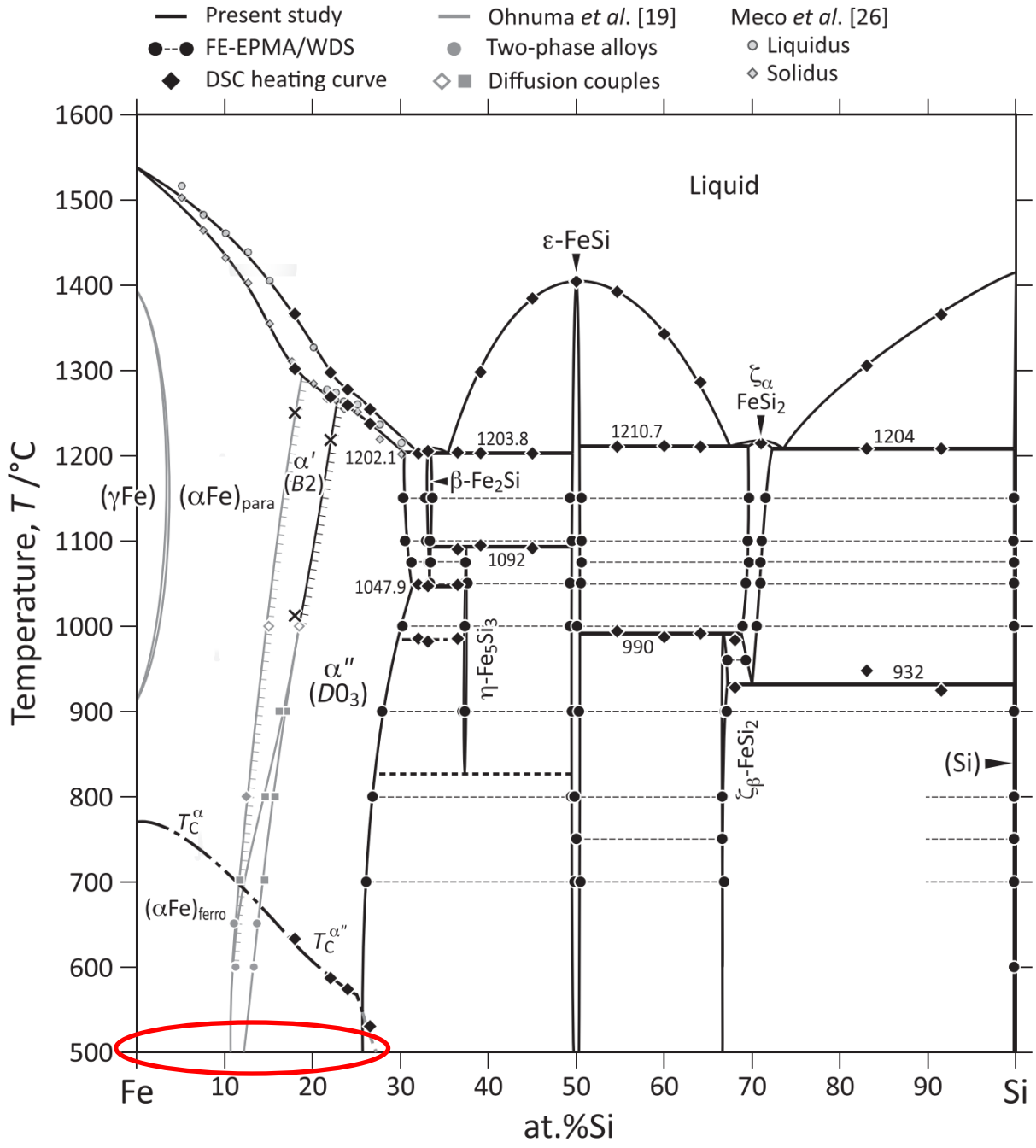


*Fig. 1: experimental phase diagram by Han et al. The region of interest in this project is indicated.*

The region in which we are interested in this project is the interval between 0 and 25 at.% (0 and 14.36 wt.%): the left-hand side of this interval is pure iron, and the right-hand side is $Fe_3Si$. Both crystals have in common that iron and silicon atoms are distributed over an underlying body-centered cubic (bcc) lattice – there will be small local position adjustments based on the details of the local configuration, but globally spoken there is a bcc lattice that is decorated by Fe and Si atoms. This is experimentally known to be true for the entire interval (0-25 at.%).

In the region of 11-13 at.% (5.85-6.99 wt.%), this phase diagram shows a two-phase alloy of iron with some randomly dispersed Si atoms and ordered $Fe_3Si$ crystals (DO3 structure). At higher temperatures, there is a B2 phase (another ordered decoration of the bcc lattice, with 50% Fe and 50% Si). The experimental phase diagram does not extend down to room temperature or to the ground state near absolute zero, but by extrapolation, it looks like a line compound could be found around 11 at.%. The phase diagram at the right has this low temperature region included, with an extrapolation to how the phases would look like at the lowest temperatures.

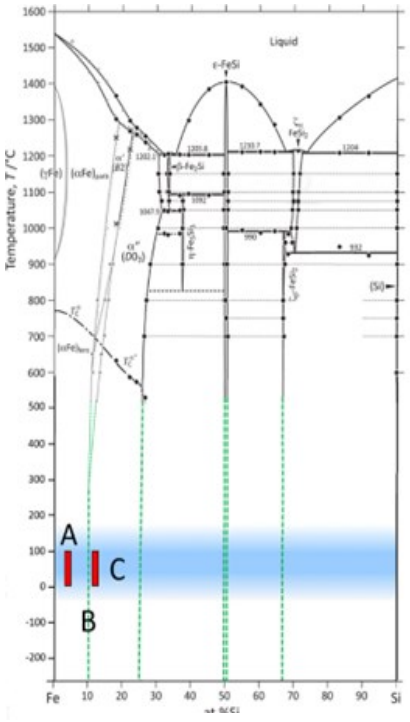


*Fig. 2: experimental phase diagram extrapolated to the ground state (copy from the project proposal). The shaded zone indicates the region around room temperature, which should be similar to the ground state behaviour.*

The region of 11 at.% is right into the technologically interesting interval of 5.8-12.1 at.% (3-6.5 wt.%) for Fe-Si electrical steels. Current electrical steels have a composition at the lower end of this interval. For their electromagnetic properties, steels at the higher end would be more suitable. They turn out to be mechanically brittle, however, and cannot easily be machined. It is not clear where this comes from, and therefore an important part of the Si-Shift project is to examine what exactly is happening with the structure of Fe-Si alloys in this area. This will be done by ab initio quantum simulations, at 0 K.

## 2 Computational methodology

Fe-Si alloy crystal structures were created from a bcc-lattice for which all atom positions were occupied by either iron or silicon atoms. Both the Si-concentration (expressed in at.% or wt.%) and the relative positions of all atoms are degrees of freedom and can be varied. The number of bcc sites that lie in the volume that is taken as unit cell determine which concentrations and which relative positions are accessible.

At the left-hand side of the considered interval (0 at.%) we have pure bcc-iron (ferrite). All bcc positions are occupied by Fe atoms. At the right-hand side of the considered interval (25 at.%), we have the $Fe_3Si$ stoichiometry. This crystal is experimentally known. It has a (conventional) unit cell of 16 atoms (2x2x2 =

8 bcc cubes), of which the body center atoms of 4 bcc cubes are occupied by Si atoms, in a way that they form a regular tetrahedron.

With a cell of 16 atoms, concentration steps of 1/16 (=6.25 at.%) can be made. This means we can study with this cell only the alloys with 0 at.%, 6.25 at.%, 12.5 at.%, 18.75 at.% and 25 at.%. In order to study intermediate concentrations, larger cells are required. In the present report, we used cells with up to 250 atoms (concentration steps of 0.4 at.%).

For a given cell size and a given concentration, there are many ways to decorate the lattice with the given number of Fe and Si atoms, and many of these are essentially identical because they can be transformed into one another by symmetry operations. The `Supercell` code (https://doi.org/10.1186/s13321-016-0129-3) was used to select all inequivalent decorations. The table lists the number of inequivalent cases for cells that are multiples of the primitive bcc cell.

*Tab. 1: inequivalent cases for multiples of the primitive bcc cell, in the Si-concentration range of interest*

| # bcc sites per cell | nxnxn | # Si atoms | Si concentration (at.%) | # inequivalent structures |
|---|---|---|---|---|
| **8** | 2x2x2 | 1 | 12.5 | 1 |
| | | 2 | 25.0 | 3 |
| **27** | 3x3x3 | 1 | 3.7 | 1 |
| | | 2 | 7.4 | 5 |
| | | 3 | 11.1 | 20 |
| | | 4 | 14.8 | 84 |
| | | 5 | 18.5 | 308 |
| | | 6 | 22.2 | 1052 |
| **64** | 4x4x4 | 3 | 4.7 | 82 |
| | | 4 | 6.3 | 1028 |
| | | 5 | 7.8 | 10474 |
| | | 6 | 9.4 | 100293 |
| | | 7 | 10.9 | 815687 |
| | | 8 | 12.5 | 5788777 |
| | | 9 | 14.1 | 35919251 |
| | | 10 | 15.6 | 197412521 |
| | | 11 | 17.2 | 968607702 |
| **125** | 5x5x5 | 5 | 4.0 | 158989 |
| | | 6 | 4.8 | 3144856 |
| | | 7 | 5.6 | 53237604 |
| | | 8 | 6.4 | 968607702 |
| | | 9 | 7.2 | 784520350 |
| | | 10 | 8.0 | 3018326790 |

As the table shows, there are thousands of billions of possibilities. Each case takes a couple of minutes to hours to process by quantum simulations, and therefore it is not feasible to run all cases. A (very limited) choice has to be made. Some sets with a limited number of atoms (8, 27) were screened exhaustively, and based upon the patterns that emerged from this as low-energy cases, variants in larger cells were tried. A total of 535 cases are considered for this report.

Total energies of all considered cells were computed by the Density Functional Theory (DFT) code VASP. The PBE exchange-correlation functional was used, with PAW_PBE Fe_GW and PAW_PBE Si_GW as pseudopotential files for Fe and Si. To determine precise computational settings, benchmark calculations were performed on a crystal with 16 atoms, with the number of silicon atoms varying from one to three. This process led to the selection of a basis set size characterized by ENCUT=600 eV, a 9×9×9 k-point mesh (for a 16-atom cell, this is equivalent to a 13x13x13 mesh for an 8-atom cell or a 4x4x4 mesh for a 250-atom cell) and EDIFF=$10^{-7}$ eV for the SCF convergence. Geometry optimization was terminated by the criterion of the forces converging to less than 0.02 eV/Å (EDIFFG = -0.02).

*Figure 3. Sample VASP input file (INCAR)*

```
INCAR:
  ALGO = Fast
  NCORE = 32
  KPAR = 1
  EDIFF = 1E-7
  ENCUT = 600
  IBRION = 2
  ISMEAR = 2
  ISIF = 3
  ISPIN = 2
  LASPH = .TRUE.
  LMAXMIX = 4
  LORBIT = 11
  LREAL = .FALSE.
  LWAVE = .FALSE.
  MAGMOM = 3*0.6 24*0.6
  NELM = 100
  NSW = 99
  PREC = Accurate
  SIGMA = 0.2
  NWRITE = 1
  NELMIN = 4
  EDIFFG = -0.02

POTCAR:    PAW_PBE Si_GW 04May2012
POTCAR:   PAW_PBE Fe_GW 31Mar2010
```

Using the total energies that were obtained this way, the formation energy for every crystal could be expressed with respect to bcc-Fe and DO3. Values are reported per atom. Positive formation energies mean that energy is required to transform the suitable mixture of bcc-Fe and DO3 into the considered

alloy. Negative formation energies indicate that the alloy will spontaneously form if a suitable amount of bcc-Fe and DO3 is mixed.

## 3 Dissolving a single Si atom in an iron matrix

An elementary step in the analysis of the 535 formation energies is answering the question: "*How much energy does it cost to replace one Fe atom in an infinitely large bcc lattice?*" The limit of an infinitely large bcc lattice corresponds to the limit of 0 at.% Si concentration. We cannot reach this limit, but we can approach it by taking ever larger cells, where exactly one Fe atom is replaced by Si. There are 9 such cases available in our data set (cell sizes of 8, 16, 27, 54, 64, 125, 128, 216 and 250 atoms, respectively). They represent the concentration range of 12.5 to 0.4 at.%.

Fig. 4 shows this energy cost as a function of the Si concentration. Large Si concentrations (small cells) are at the right, and small Si concentrations (large cells) are at the left. One expects some scatter in the data for large concentrations, as the periodic copies of the Si atom will interact with each other. When lowering the concentration, the periodic copies are further and further apart from each other and do not interact any more. This represents the limit of introducing a truly isolated Si atom. Globally, this trend is present in Fig. 4, with a value of about 0.11 eV as energy cost to introduce an isolated Si atom into the iron lattice. There are two exceptions for concentrations of 3.7 and 0.46 at.% (27 and 216 atoms), marked by arrows in Fig. 4. These turn out to be 'resonances', where the distance between the periodic copies is just right to lower (27 atoms) or increase (216 atoms) the formation energy. One strong argument for this is that the distance between two Si atoms in the 216-atom cell is exactly twice as large as in the 27-atom cell. The cell with 27 atoms will represent a particularly stable alloy (see Sec. 5 and Sec. 6).

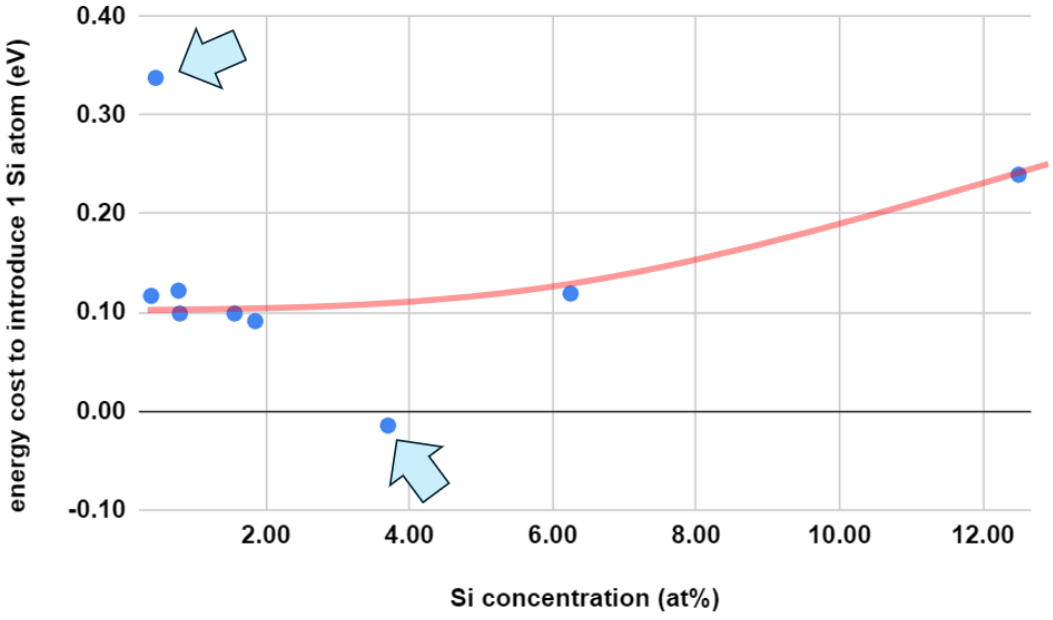


*Fig. 4. Energy cost to introduce one Si atom in a iron matrix, as a function of the number of atoms in the unit cell (or effective Si concentration). The red line is a guide to the eye. Two cases that deviate from the trend are indicated by an arrow.*

## 4 Dissolving a Si-Si pair in an iron matrix

The next step in the analysis is examining the interaction between two otherwise isolated/diluted Si atoms in a bcc iron lattice. *Will they attract or repel each other?* We examine this by selecting from our 535 cases those with 2 Si atoms and plot the energy cost to bring these into the iron lattice, as a function of the distance between the Si atoms. The 5 distances in the plot are the 1st, 2nd, 3rd, 4th and 5th nearest neighbour distances. Data are plotted for cells with 54, 64 and 128 atoms. For the smallest cells, there can be more interaction between the periodic copies, and therefore the cell with 128 atoms represents the best approximation for the Si-Si interaction in an infinite lattice. The green line represents the energy of two isolated Si atoms, i.e. 2x the 0.11 eV that was obtained from Fig. 4.

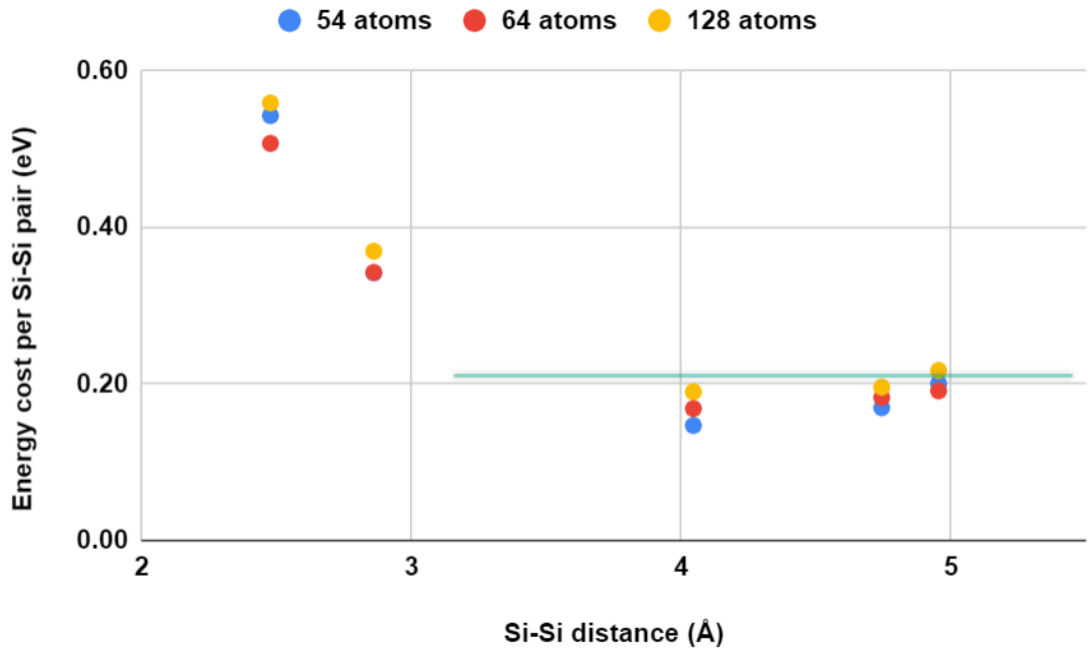


*Fig. 5 Energy cost per Si-Si pair as a function of Si-Si distance for 3 cell sizes. The green line represents the energy of two isolated Si atoms (2x 0.11 eV, see Fig. 4).*

From this figure, it can be concluded that Si atoms repel each other when they come close together (1st and 2nd nearest neighbour distances). When the two Si atoms are 5 nearest neighbour distances apart, the energy is close to the energy of two independent Si atoms, and we can conclude that the two Si atoms do not interact any longer. There is a shallow minimum for the 3rd and 4th nearest neighbour distances. We will indeed see that Fe-Si alloys with favourable formation energies will aim for a Si network that maximizes the number of Si-Si pairs with these distances. This is consistent with the DO3 structure – which does appear in nature – for which every Si atom is at a 3th nearest neighbour distance of 4 other Si atoms.

## 5 Screening more concentrations and configurations

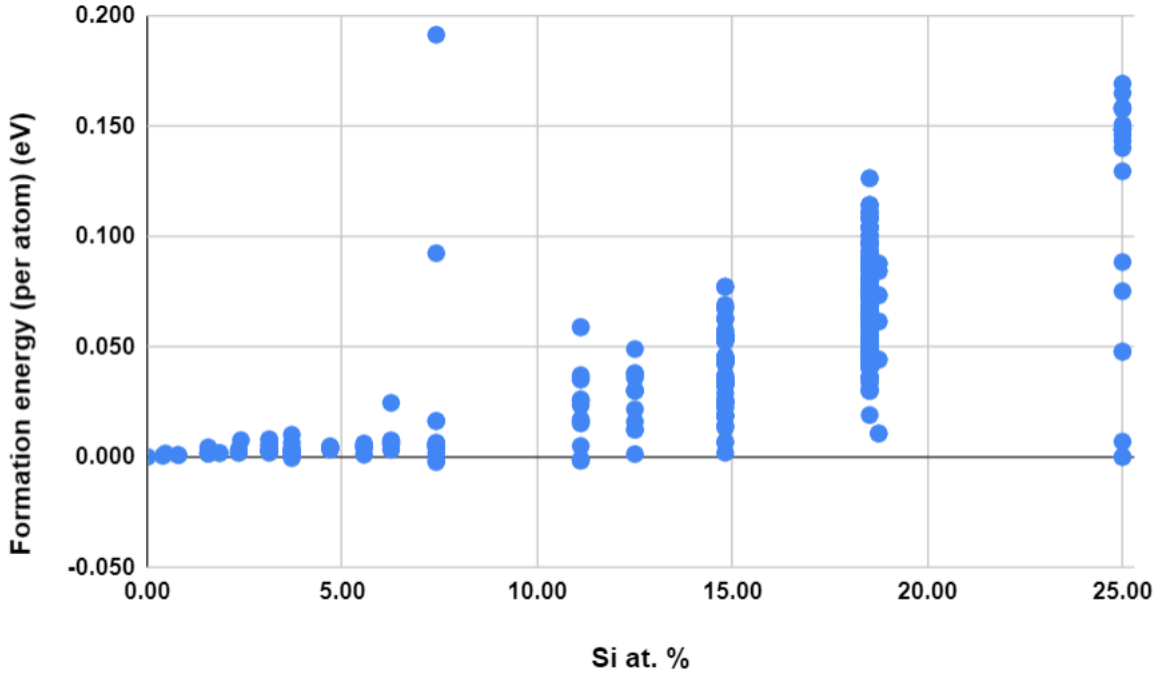


*Fig 6. Formation energy per atom vs. silicon concentration for all 535 studied alloys*

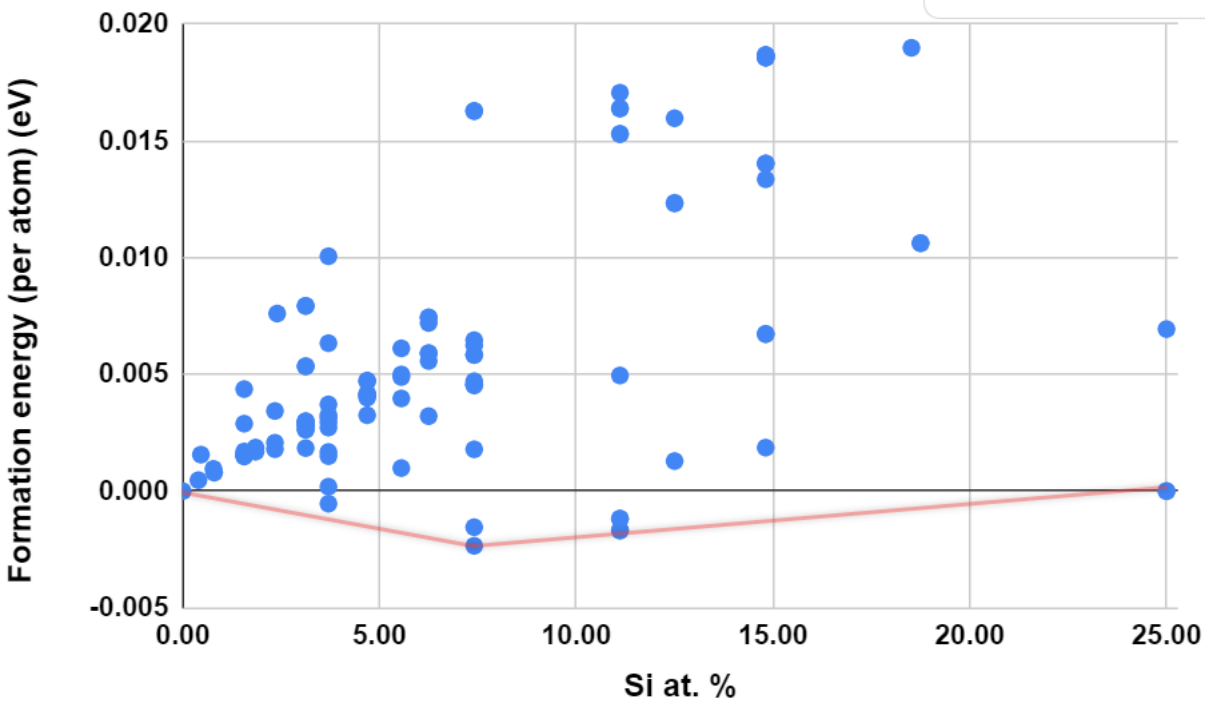


*Fig. 7 : same as Fig. 6, but zoomed in on the relevant region for negative and near-zero formation energies.*

The formation energies for all 535 studied cases are shown in Figs. 6 and 7 (in the latter, formation energies larger than 0.02 eV are not shown, because these alloys are definitely not stable). All crystals with a negative formation energy are more stable than a combination of bcc-Fe and DO3. The red lines represent a convex hull construction, which is the procedure to identify the crystals that are absolutely stable: they cannot lower their energy by splitting themselves in combination of other crystals on the plot. There turn out to be three stable crystals: bcc-Fe and DO3 (both of them are experimentally known), plus another one at 7.4 at.% Si that has not been mentioned before in the literature. Because this concentration is close to the region where in the experimental phase diagram the B2 phase appears, we put forward the hypothesis that this newly identified alloy is the one that appears in nature but has not been correctly characterized in the experiments that lead to the construction of the phase diagram. There are many arguments to be given to support this hypothesis. They will be listed elsewhere, here we will mention only one very obvious one: the B2 crystal structure requires 50 at.% Si, and can therefore not be consistent with this concentration range.

The newly identified crystal has space group Fmmm, and can be characterized as follows: the Si atoms are in (110) planes, separated from the next Si-containing plane by 2 pure Fe layers. Within their plane, the Si atoms form 3$^{th}$ and 4$^{th}$ nearest neighbour pairs (marked by red and black lines in Fig. 8).

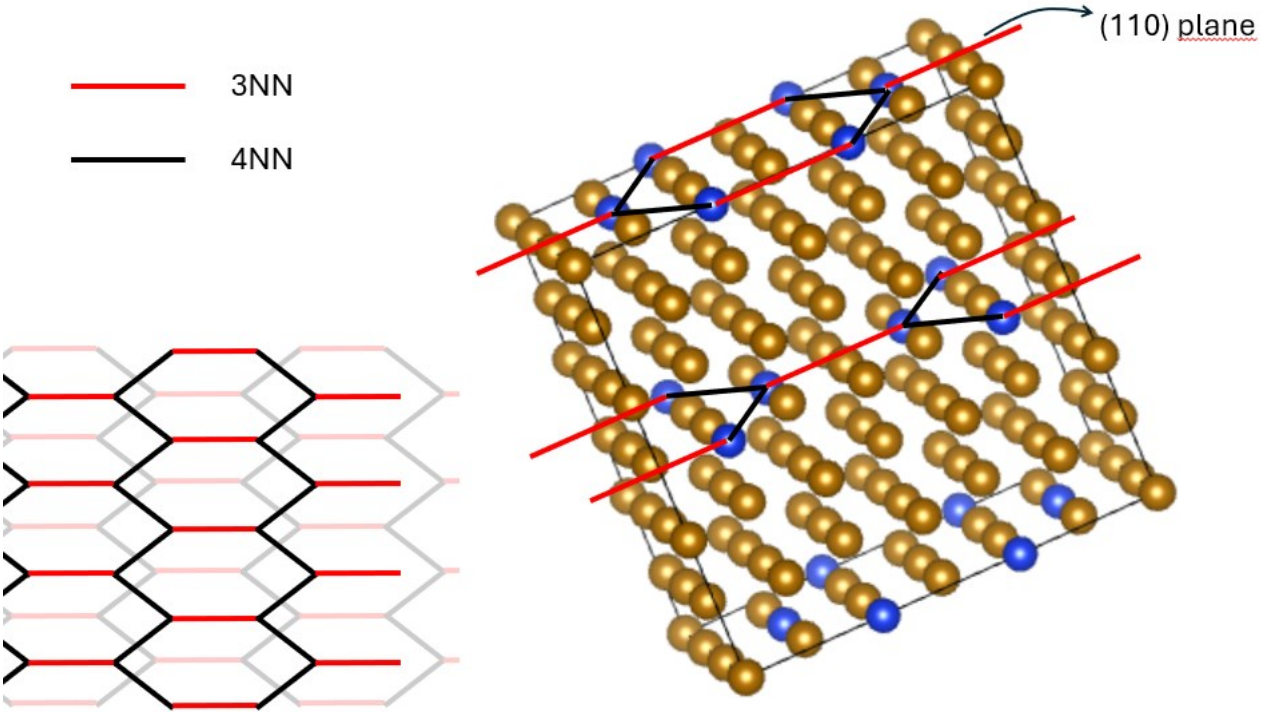


*Fig 8. The newly identified crystal structure*

## 6 Conclusion

Based on this extensive computational screening, we put forward a new interpretation of the Fe-Si phase diagram, for the ground state structures in the 0-25 at.% Si interval :

- There are three line compounds:
  - bcc-Fe at 0 at.% Si
  - the new Fmmm crystal at 7.41 at.% Si
  - DO3 at 25 at.% Si

- There are two mixed-phase regions:
  - Alloys with a Si concentration between 0 and 7.41 at.% will separate into a concentration-conserving mixture of bcc-Fe and Fmmm
  - Alloys with a Si concentration between 7.41 and 25 at.% will separate into a concentration conserving mixture of Fmmm and DO3.